

Predicting ECAP misorientation evolution and its influence on superplasticity for an Al-Zn-Mg-Cu alloy

Fernando Carreño *

Dpt. Physical Metallurgy, CENIM, CSIC, Av. Gregorio del Amo 8, 28040 Madrid, Spain

carreno@cenim.csic.es

Keywords: Aluminium SPD Grain Refinement, ECAP Misorientation Evolution, New Misorientation Expression, GBS Superplastic Constitutive Equation

Abstract. Extensive research on severe plastic deformation (SPD) of metallic materials has been performed so far in order to improve mechanical properties, both at low and high temperatures. As a result of the extensive grain refinement obtained, increased superplastic behaviour has been attained at higher strains rates and lower temperatures than usual. This is due to finer grain sizes and higher average misorientations obtained, which enhance grain boundary sliding (GBS). However, the misorientation effect on superplasticity, and the prediction of misorientation evolution during SPD has remained so far, qualitative. In this research, especial attention has been given to the quantitative misorientation evolution with increasing equal channel angular pressing (ECAP) deformation, in order to propose an expression useful to describe and predict the influence of the different processing parameters on the misorientation evolution with strain. This is exemplified for ECAPed Al-Zn-Mg-Cu and other aluminium alloys, and it could serve as a basis for predicting the misorientation evolution, and its influence on superplasticity, of other SPD processes and metallic alloys.

Introduction

Widespread research on severe plastic deformation (SPD) of metallic materials has been performed in order to improve mechanical properties, both at low and high temperatures as a result of the extensive grain refinement obtained [1-15]. At low temperatures, high yield and ultimate tensile stresses, as well as higher than usual ductility is found, increasing toughness. At high temperatures, increased superplastic behaviour has been attained at higher strain rates and lower temperatures than usual due to finer grain sizes, L , and higher average misorientations, $\bar{\delta}$, which enhance grain boundary sliding (GBS) mechanism [8-9,11-16]. However, the misorientation effect on superplasticity has not been studied as much as the effect of grain size. In this research, a tool for description, analysis and prediction of the misorientation evolution with increasing applied strain is proposed, which will be useful to predict superplastic behaviour with higher accuracy.

Equal channel angular pressing (ECAP) is a severe plastic deformation processing technique consisting in a die having two channels, of equal cross section, intersecting at an angle, typically 90°, or 120°. It was first described by Segal et al. [1]. In an ECAP, ideally, a billet experiences simple shear without a change in cross-sectional area while it is pressed through, and so, the pressing may be repeated many times. As a consequence, large cumulative plastic strains can be introduced to a billet in multi-pass ECAP processing. This processing leads in metals and alloys to microstructure refinement and the development of ultra-fine and nanoscale grains. Additionally, during multi-pass ECAP the strain-path can be varied by choice of processing route, for instance, route A, B_A, B_C or C, etc., differing in the sense of billet rotation in between successive pressing passes. B_C (rotating 90°) and A (no rotations) are the most common routes.

An interesting feature of ECAP processing is that, for a 90° or 120° ECAP, one pass is approximately equivalent to a true deformation (ϵ) value of 1 or 0.7, respectively, being necessary

at least 12 or 16 passes to obtain highly misoriented microstructures. Therefore, ECAP allows convenient study of microstructure evolution as a function of applied strain. Additionally, ECAP allows proper measuring of processing stress [7-8, 11] and adequate temperature control. Generally, the lower the ECAP temperature, the finer the microstructure and the slower the microstructural evolution towards highly misoriented ultrafine grains. Another factor affecting the microstructure evolution during ECAP processing is the composition of the alloy, which may have precipitates and/or solutes in solid solution.

Although the mechanisms of microstructure evolution are an important subject, they are not in the scope of this article. This work will focus in the description of the misorientation evolution irrespective of the underlying microstructural mechanism. Preferably, it is convenient not to have discontinuous behaviour such as given by discontinuous recrystallization, or abnormal grain growth between ECAP passes. The ideal situation would be that corresponding, approximately, to a continuous dynamic recovery (CDRV), for which all the deformation will be employed in increasing progressively the misorientation of the ultrafine subgrains, which were obtained in the initial passes. It must be noted that this is not the general situation, because usually, certain progressive refinement is occurring even for a high number of passes.

Nevertheless, the objective of this work is to offer an adequate tool for the description, analysis and prediction of the misorientation evolution during increasing number of ECAP passes, i.e., as a function of applied strain.

Proposed tool for misorientation evolution study

For metallic materials being processed by SPD, the misorientation evolution with applied strain can be divided in three stages: i) the initial vast grain subdivision from coarse grain to fine or ultrafine subgrains with low angle grain boundaries, LAGBs (Stage I), ii) the approximately linear increase of average subgrain misorientation, gradually, towards high angle grain boundaries, HAGBs (Stage II), and iii) the final slow and asymptotic behaviour towards a maximum average misorientation (Stage III). The three stages have already been reported by other researchers [5]. This maximum average misorientation, $\bar{\delta}_{\max}$, should correspond, ideally, to the average misorientation of a random distribution, $\bar{\delta}_{\max} = \bar{\delta}_{\text{random}}$, as described by Mackenzie, which is $\bar{\delta}_{\text{random}} = 41^\circ$ for cubic metals and alloys [17].

An important idea to highlight in this work is that the final slow misorientation increment with applied deformation is not attributed, in principle, to any recrystallization mechanism, but just the result of being close to a total misorientation randomization. Of course, any possible recrystallization process could accelerate the randomization process or even change the final result with unexpected misorientation distributions. Anyway, the tool proposed below will help in the description and analysis of the underlying mechanisms. In this work, it won't be considered, nor predicted, the initial grain subdivision, just characterized by a "zero point" parameter, designated k_0 , as it will be shown in the following.

The tool takes into account two facts: i) the initial misorientation increments of the newly formed subgrains behave approximately linear with applied deformation, and ii) the final misorientation increments of the grains are small for large applied strains, trending to an asymptotic value. For these reasons, it is proposed the use of the arctan function ($\bar{\delta} \approx \arctan(f(\epsilon))$), which meets these features. In this way, we can concentrate our future analysis in the argument, $f(\epsilon)$, to get insights about the influence of different microstructural and processing parameters, such as grain size, precipitates, solid solution, stacking fault energy (SFE), ECAP geometry (90° , 120°), processing route (A, B_C), temperature (RT, HT), etc.

The arctan function presents an initial positive linear slope from zero value, and asymptotic behaviour for high argument values. With just two parameters, k_1 and k_2 , it can describe quite different Stages II (linear) and III (asymptotic). It can be added another parameter, k_0 ,

characterizing a starting point depending on the Stage I (initial subgrain subdivision). This function, in terms of average misorientation vs. applied strain is given by:

$$\bar{\delta} = \bar{\delta}_{random} \left(\frac{2}{\pi}\right) \arctan\left(\left(\frac{\pi}{2\bar{\delta}_{random}}\right) k1 (\epsilon - k0)^{k2}\right) \quad (1)$$

where $\bar{\delta}$ is the average misorientation, $\bar{\delta}_{random} = 41^\circ$ for cubic metals and alloys, as derived by Mackenzie [17], ϵ is the total applied true strain, $k0$ is the “zero point” parameter (to obtain the fine initial subgrains, the “zero point” for counting the strain in Stage II), $k1$ can be regarded as a misorientation rate, and $k2$ as an effectiveness parameter. We put inside arctan the value “ $(\pi/2\bar{\delta}_{random})$ ” because we had to put outside its inverse to get the asymptotic value of $\bar{\delta}_{random}$ at high strains, and the initial slope = $k1$. In principle, the expected values of the parameters are around $k0 \approx 1-2$, $k1 \approx 6$ and $k2 \approx 1$. This means that we expect about one or two ECAP passes to obtain the initial ultrafine subgrains with minimum misorientation ($k0 \approx 1-2$), an increase of average misorientation of 6° per pass ($k1 \approx 6$), and a “typical” effectiveness ($k2 \approx 1$). The value $k2 = 1$ means that the average misorientation increases linearly with applied strain at small-medium misorientations. This is expected for a constant (sub)grain size. However, there is a tendency for decreasing grain sizes with increasing strain that may influence the experimental values of Eq.1 parameters.

Relationship between %HAGB and $\bar{\delta}$

The misorientation can be described in several ways. Histograms can be complicated when performing comparisons. Although not very precise, the simplest and most common misorientation parameters are the fraction of HAGBs, %HAGB, and average misorientation, $\bar{\delta}$. The author prefers the latter, $\bar{\delta}$, because there is only one average, $\bar{\delta}$, value from a given histogram. On the contrary, for the %HAGB, an arbitrary threshold should be established between low and high angle boundaries to calculate its value (usually 15°). Nevertheless, an approximately linear relation can be found to relate both parameters in a wide range of %HAGB or $\bar{\delta}$ [6, 9]. Therefore, to compare the different alloys data, from distinct research works, and show them in useful plots, it is convenient to make explicit the relation between $\bar{\delta}$ and %HAGB. The simplest translation should follow the expression:

$$\bar{\delta} = a + b \%HAGB \quad (2)$$

where approximate values of a and b are about $a \approx 6^\circ$, $b \approx 0.36$, for cubic metals and alloys. Other approximate values are $a \approx 4^\circ$, $b \approx 0.395$, fitted from [6], or $a \approx 5.5^\circ$, $b \approx 0.352$, fitted from [9]. Following the Mackenzie random distribution and having in mind that for %HAGB = 100%, $\bar{\delta} > \bar{\delta}_{random}$, values of $a = 6^\circ$ and $b = 0.36$ have been chosen as quite reasonable. However, each experimental misorientation histogram is different and the extreme values could show some dispersion.

Microstructure evolution during ECAP of aluminium alloys

Several examples of misorientation evolution have been taken from the literature. Some of them use $\bar{\delta}$ values, but most use the fraction of high angle boundaries, %HAGB. An example of ECAP processing at room temperature (RT) for pure Al (99.99%) up to 12 passes is given by Kawasaki et al. [6] with a 90° ECAP route B_C, rod of 10 mm diameter, 60 mm length. Each pass applied a true strain of 1. Initial grain size, L , was about 1 mm. The values of grain size, L , and misorientation, $\bar{\delta}$, are plotted together in Fig.1a up to a total strain $\epsilon = 12$.

Fig.1b shows data from Apps et al. [3] using a 120° ECAP at room temperature following Route A (without rotation) to process Al-0.13Mg and AA8079 alloys up to a strain $\epsilon = 10$ (upper axis).

In Fig.1b, it is shown that the aluminium alloy containing some coarse precipitates needs less ECAP passes to obtain similar microstructure evolution.

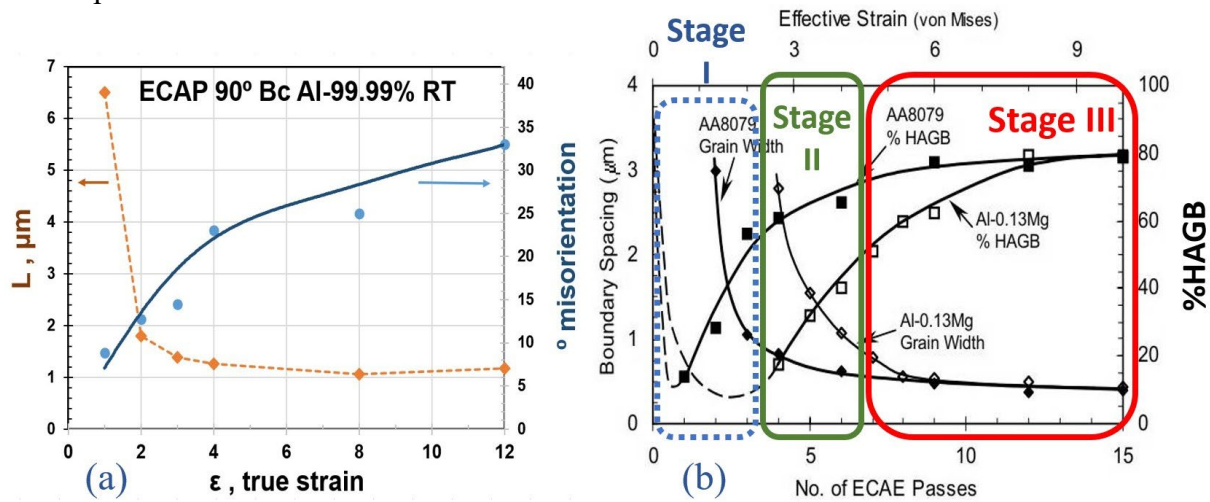


Fig.1. L and $\bar{\delta}$ vs. ϵ for a) ECAPed 90° RT pure Al (99.99%) [6] and b) ECAPed 120° RT Al-0.13Mg and AA8079 alloys [3]. Stages I, II and III are also highlighted.

Additionally, in this Fig.1b, it can be clearly shown the three stages for the misorientation evolution during ECAP. The first, Stage I, having different span depending on the alloy composition, relates to the fine subgrain initial subdivision. Following, Stage II is associated to the approximately linear misorientation increase of the fine subgrains (LAGBs) towards HAGBs. Finally, Stage III shows the asymptotic behaviour of the average misorientation as a function of applied strain. In these two alloys, the final grain size is smaller than that for the Al 99.99% alloy.

For other Al alloys including precipitates and/or elements in solid solution, an approximately similar shape of curves is obtained, although the misorientation rate is different. Fig.2 shows data for alloy AA6060-T6 processed under ECAP 90° following Route B_C at room temperature [10]. As expected, composition can make a difference in the misorientation evolution. In this case also, the final grain size is smaller than for the Al 99.99% alloy.

Regarding the behaviour of Al-Zn-Mg-Cu alloys, similar to AA7075, Goloborodko et al. [4] have performed ECAP 90° on alloy AA7475 following route A, at 523 and 673K (HT), and compared to other Al alloys, as shown in Fig.3a. The misorientation evolution of AA7475 follows the three stages, as other Al alloys (Al-0.1Mg, Al-0.13 Mg, Al-0.3Mn, Al-3Mg and AA5052). Some variations may arise by the use of a different ECAP Route, or temperature, as

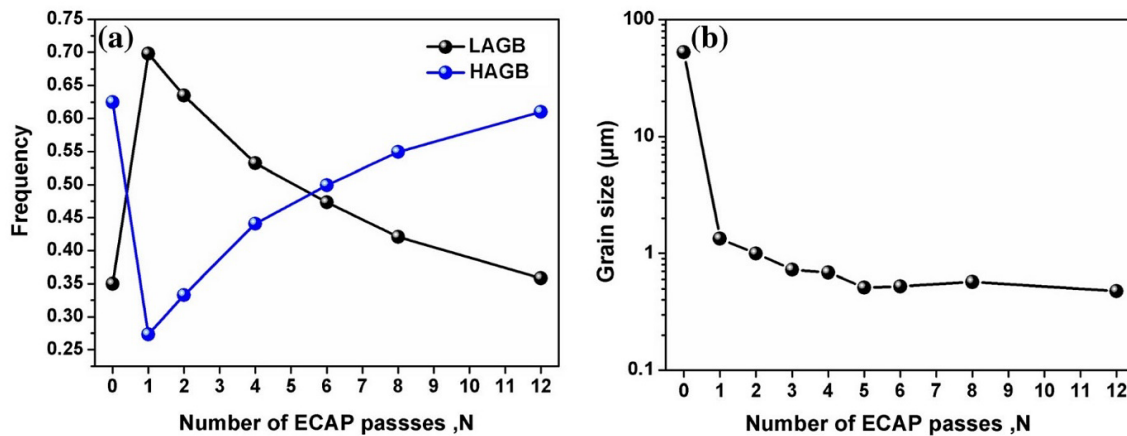


Fig.2. ECAPed 90° B_C RT AA6060-T6 Al-Mg-Si alloy [10]: a) LAGB and HAGB, and b) L (μm) vs. N (true strain).

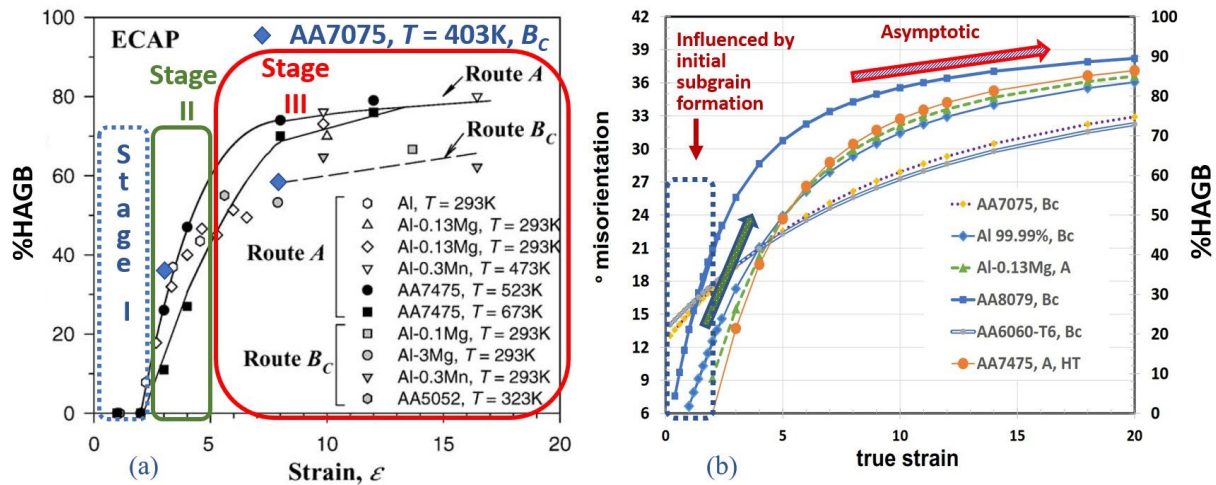


Fig.3. a) AA7475 %HAGB vs. strain compared to other Al alloys [4], and b) calculations from Eq.1 with parameters from Table 1.

Table 1. Eq.1 parameter values associated to various Al alloys, and corresponding calculations of $\bar{\delta}$ and %HAGB (Eq.2) for $\epsilon = 8$.

Alloy	k0	k1	k2	ϵ	$\bar{\delta}$	%HAGB
Al 99.99%	0.00	6.8	1	8	29.3	65
Al-0.13Mg	0.80	8.0	1	8	29.9	67
AA8079	-0.25	12.0	1	8	34.3	79
AA6060-T6	-5.00	3.0	1	8	25.6	55
AA7475 HT	1.35	9.0	1	8	30.3	68
AA7075	-4.00	3.4	1	8	26.1	56

well as composition. Additionally, Fig.3a shows data from an overaged AA7075 ECAPed 90° at 130 °C (403K) using Route B_C (37% and 56% HAGB at 3 and 8 passes, respectively, shown as the large blue coloured diamonds) [7-8]. For this AA7075 overaged alloy, grain size values diminished as ECAP passes were applied, from about 200 to 163 nm, in the shortest grain axis (transverse), for 3 and 8 ECAP passes, respectively, in line with the decline observed also by Goloborodko et al. [4]. In the case of AA7075 alloy, although only two points are available, a tentative prediction and comparison with other alloys will be performed.

Fig.3b shows the approximate misorientation evolution curves of the analysed ECAPed alloys as described using Eq.1. They will be explained in the next paragraph.

Description and predictions of misorientation evolution

To have easy and clear comparisons among alloys, the arctan function of Eq.1 will be used with only two parameters, setting the parameter k2 to 1. This is equivalent to say that misorientation increases linearly with applied strain in Stage II. This should be the ideal situation if grain size remains stable. Although it is not the real case, it is useful for approximate descriptions and comparison among different alloys. The parameter k0 corresponds to the “zero point” of Stage II and k1 gives the initial misorientation rate, as shown in Table 1 for the six alloys considered. Additionally, $\bar{\delta}$ and %HAGB values given by Eq.1 and Eq.2, respectively, for $\epsilon = 8$ are included.

Observing Table 1 and Fig.3b it can be noticed that Al 99.99% behaviour is in the middle. Its k1 = 6.8 is between 3 (AA6060-T6, full of small precipitates) and 12 (AA8079, with some coarse precipitates). Similar behaviour to AA6060-T6 shows the AA7075 alloy, having the slowest misorientation rates, probably due to their ultrafine grains still evolving. Close to the average behaviour, that of Al 99.99%, are the dilute alloy Al-0.13Mg, and the AA7475 HT ECAPed at

high temperature by Route A. The processing at high temperature helps also in the formation of HAGBs. Additionally, Route A may be more effective than Route B_C because B_C is cyclic every 4 passes. From this comparison it is clear that having a clean matrix with some fraction of non-fine precipitates helps in the development of a highly misoriented microstructure, as pointed out by Apps et al. [3].

Regarding the expected superplastic behaviour of the ECAPed alloys, interesting questions arise: When a fine, but non-randomly misoriented, grain structure will be superplastic? And, if so, in what extent?

Influence of misorientation on superplastic behaviour

Superplasticity at intermediate-high temperatures is obtained thanks to the operation of the grain boundary sliding (GBS) mechanism. As a consequence, it is necessary a fine, equiaxed and highly misoriented grain structure. In fact, the finer, the more equiaxed and the more misoriented the grain, the better. During decades, several phenomenological, although similar, constitutive equations have been proposed, but they do not contemplate the misorientation as an explicit parameter [8, 14, 16]. The only attempts to obtain a superplastic equation including explicitly the fraction of HAGBs (%HAGB) or average misorientation ($\bar{\delta}$) are recent [9, 12-13]. In [12-13] it was proposed the idea that if the average misorientation is less than random, the material behaves as if the “randomly misoriented equivalent grain size for GBS”, L_{GBSeq} , is larger than the grain size, L . This is conveniently described by expression [13]:

$$L_{GBSeq} = L (\bar{\delta}_{random}/\bar{\delta})^2 \tag{3}$$

where $\bar{\delta}$ is the experimental average misorientation corresponding to the experimental L value. Therefore, the smaller the alloy misorientation, the less superplastic. The full expression for the new superplastic GBS constitutive equation is [12-13]:

$$\dot{\epsilon} = A \left(\frac{\sigma}{E}\right)^2 \left[\left(\frac{\bar{\delta}}{\bar{\delta}_{random}}\right)^2 \left(\frac{b}{L}\right)\right]^2 \frac{D_L}{b^2} \tag{4}$$

where σ is the applied stress, E is the Young Modulus, b is the Burger’s vector, D_L is the coefficient of lattice self-diffusion and A is a material constant.

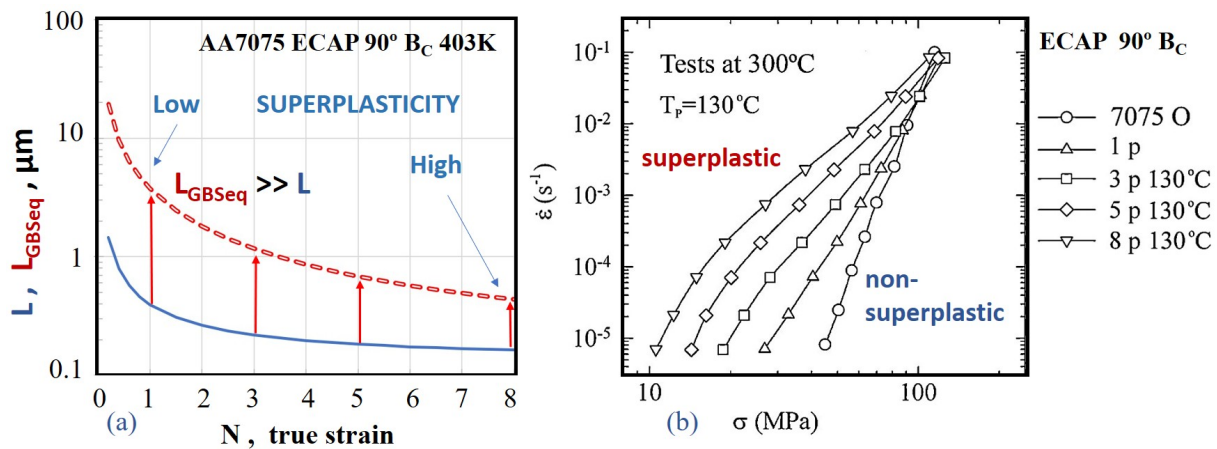


Fig.4. a) L and L_{GBSeq} vs. ϵ for ECAPed AA7075 explaining b) the lesser or greater superplasticity after various ECAP passes. L and tensile test data taken from [7-8].

Now, having data of both grain size, L , and average misorientation, $\bar{\delta}$, we are able to predict the effective grain size for GBS superplastic behaviour, L_{GBSeq} . For instance, for alloy AA7075 [7]

taking into account the misorientation evolution given by Eq. 1 with parameters of Table 1, shown in Fig.3b, and L evolution with ECAP passes, shown in Fig.4a, the L_{GBSeq} values predicted by Eq.3 are shown also in Fig.4a. Additionally, Fig.4b shows strain rate-stress data at 300 °C after various ECAP passes at 130°C (403K) [8] presenting the large effect in the superplastic deformation of the GBS-equivalent grain size.

Not surprisingly, L_{GBSeq} values can be between two and ten times larger than L values, being L_{GBSeq} larger the lower the applied strain, and thus, making an important difference in superplastic behaviour from one to eight passes, as shown in Fig.4b. These predicted L_{GBSeq} values can be very useful for technical applications, such as superplastic forming in the aeronautical and aerospace industries.

Summary

- Average grain misorientation, $\bar{\delta}$, increases continuously with applied strain, ϵ , in SPD processes, such as ECAP, which is particularly useful to model the misorientation evolution because the misorientation saturation is usually found after about 12 or 16 ECAP passes.
- Initially, a network of low-misoriented subgrains should be formed (Stage I). This step could take a variable amount of strain depending on initial grain size and composition. For instance, solid solution may delay this step, whereas precipitates may favour it.
- Next, for increasing ECAP passes, generally, misorientation should increase linearly with increasing applied deformation, transforming LAGBs into HAGBs (Stage II).
- Finally, for large strains (Stage III), the average misorientation values tend to saturate asymptotically towards the Mackenzie distribution average misorientation value, $\bar{\delta}_{random}$. For cubic metals and alloys $\bar{\delta}_{random} = 41^\circ$.
- To describe and analyse the misorientation evolution with applied strain, it is proposed the use of the arctan function to take into account both the initial linear behaviour and the final asymptotic behaviour towards the misorientation saturation value. In its simpler form, it is proposed the equation: $\bar{\delta} = \bar{\delta}_{random} (2/\pi) \arctan(\pi/2 \bar{\delta}_{random} \cdot k1 \cdot (\epsilon - k0)^{k2})$, where k0, k1 and k2 are constants depending on the material and processing variables. k0 relates to the strain needed to start Stage II, k1 relates to the initial misorientation rate respect to the applied strain (in Stage II), and the exponent k2 is about 1, for a constant grain size, related to the linearity of misorientation evolution in Stage II. These parameters depend on composition, microstructure and processing parameters.
- Once the alloys have been processed, and knowing their values of grain size, L, and average misorientation, $\bar{\delta}$, “GBS-equivalent grain size” values can be obtained so that their superplastic behaviour can be adequately compared. The GBS-equivalent grain size is given by: $L_{GBSeq} = L \cdot (\bar{\delta}_{random} / \bar{\delta})^2$ [12-13]. Finally, L_{GBSeq} substitutes L in the superplastic GBS constitutive equation, thus providing more accurate predictions, having taken into account the average misorientation values.

Acknowledgements

Financial support from MINECO (Spain), Project MAT2015-68919-C3-1-R (MINECO/FEDER) is gratefully acknowledged. Funding from the project PID2020-118626RB-I00 awarded by MCIN/AEI/10.13039/501100011033 is also acknowledged. O.A. Ruano, J.M. García-Infanta, C.M. Cepeda-Jiménez and A. Orozco-Caballero are greatly acknowledged for making this work possible.

References

- [1] V. M. Segal, Plastic Working of Metals by Simple Shear, Russian Metallurgy, Vol. 1, 1981, pp. 99-105

- [2] R. Valiev, R. Islamgaliev, I.V. Alexandrov, Bulk Nanostructured Materials from Severe Plastic Deformation. *Prog. Mater. Sci.* 45 (2000) 103-189. [https://doi.org/10.1016/S0079-6425\(99\)00007-9](https://doi.org/10.1016/S0079-6425(99)00007-9)
- [3] P.J. Apps, J.R. Bowen, P.B. Prangnell, The effect of coarse second-phase particles on the rate of grain refinement during severe deformation processing, *Acta Mater.* 51 (2003) 2811-2822. [https://doi.org/10.1016/S1359-6454\(03\)00086-7](https://doi.org/10.1016/S1359-6454(03)00086-7)
- [4] A. Goloborodko, O. Sitdikov, R. Kaibyshev, H. Miura, T. Sakai, Effect of pressing temperature on fine-grained structure formation in 7475 aluminum alloy during ECAP, *Mater. Sci. Eng. A* 381 (2004) 121-128. <https://doi.org/10.1016/j.msea.2004.04.049>
- [5] I. Mazurina, T. Sakai, H. Miura, O. Sitdikov, R. Kaibyshev, Grain refinement in aluminum alloy 2219 during ECAP at 250 °C, *Mater. Sci. Eng. A* 473 (2008) 297-305. <https://doi.org/10.1016/j.msea.2007.04.112>
- [6] M. Kawasaki, Z. Horita, T.G. Langdon, Microstructural Evolution in High Purity Aluminum Processed by ECAP, *Mater. Sci. Eng. A* 524 (2009) 143-150. <https://doi.org/10.1016/j.msea.2009.06.032>
- [7] C.M. Cepeda-Jiménez, J.M. García-Infanta, O.A. Ruano, F. Carreño, Mechanical properties at room temperature of an Al-Zn-Mg-Cu alloy processed by equal channel angular pressing, *J. Alloys Compounds* 509 (2011) 8649-8656. <https://doi.org/10.1016/j.jallcom.2011.06.070>
- [8] C.M. Cepeda-Jiménez, J.M. García-Infanta, O.A. Ruano, F. Carreño, High strain rate superplasticity at intermediate temperatures of the Al 7075 alloy severely processed by equal channel angular pressing, *J. Alloys Compounds* 509 (2011) 9589-9597. <https://doi.org/10.1016/j.jallcom.2011.07.076>
- [9] K. Wang, F.C. Liu, P. Xue, D. Wang, B.L. Xiao, Z.Y. Ma, Superplastic Constitutive Equation Including Percentage of High-Angle Grain Boundaries as a Microstructural Parameter, *Metall. Mater. Trans. A* 47A (2016) 546-559. <https://doi.org/10.1007/s11661-015-3230-8>
- [10] T. Khelifa, M. A. Rezik, J. A. Muñoz-Bolaños, J. M. Cabrera-Marrero, M. Khitouni, Microstructure and strengthening mechanisms in an Al-Mg-Si alloy processed by equal channel angular pressing (ECAP), *The Int. J. Adv. Manuf. Techn.* 95 (2018) 1165-1177. <https://doi.org/10.1007/s00170-017-1310-1>
- [11] F. Carreño, O.A. Ruano, Superplasticity of Aerospace 7075 (Al-Zn-Mg-Cu) Aluminium Alloy Obtained by Severe Plastic Deformation, *Defect Diff. Forum* 385 (2018) 39-44. <https://doi.org/10.4028/www.scientific.net/DDF.385.39>
- [12] A. Orozco-Caballero, O.A. Ruano, E. F. Rauch, F. Carreño, Severe friction stir processing of an Al-Zn-Mg-Cu alloy: Misorientation and its influence on superplasticity, *Mater. Design* 137 (2018) 128-139. <https://doi.org/10.1016/j.matdes.2017.10.008>
- [13] F. Carreño, A. Orozco-Caballero, Superplastic GBS Constitutive Equation Incorporating Average Grain Misorientation Dependence, *Mater. Sci. Forum* 941 (2018) 1501-1506. <https://doi.org/10.4028/www.scientific.net/MSF.941.1501>
- [14] R.B. Figueiredo, M. Kawasaki, T.G. Langdon, Seventy years of Hall-Petch, ninety years of superplasticity and a generalized approach to the effect of grain size on flow stress, *Prog. Mater. Sci.* 137 (2023) 101131. <https://doi.org/10.1016/j.pmatsci.2023.101131>
- [15] K. Edalati, Superfunctional Materials by Ultra-Severe Plastic Deformation, *Materials* 16 (2023) 587. <https://doi.org/10.3390/ma16020587>
- [16] O.A. Ruano, O.D. Sherby, On constitutive equations for various diffusion-controlled creep mechanisms, *Rev. Phys. Appl.* 23 (1988) 625-637. <https://doi.org/10.1051/rphysap:01988002304062500>
- [17] J.K. Mackenzie, Second Paper on Statistics Associated with the Random Disorientation of Cubes, *Biometrika* 45 (1958) 229-240. <http://www.jstor.org/stable/2333059>